Experimental demonstration of the frequency dependence of the effective scatterer number density

Jian-Feng Chen,[a] James A. Zagzebski, and Ernest L. Madsen
Department of Medical Physics, University of Wisconsin—Madison, Madison, Wisconsin 53706

(Received 19 June 1995; revised 18 October 1995; accepted 25 October 1995)

In previous papers, a data reduction method for determining a frequency-dependent "effective scatterer number density" in ultrasound was reported [Chen *et al.*, J. Acoust. Soc. Am. **95**, 77–95 (1994); **96**, 2556–2563 (1994)]. The effective scatterer number density is the actual number density of scatterers multiplied by a frequency-dependent factor that depends on the differential scattering cross sections of the scatterers. Evaluation of this technique based on measurements applied to a phantom with a distribution of scatterer diameters is reported here. This condition yields an effective scatterer number density that depends on the dominant scatterer concentration at the analysis frequency. Measured scatterer number densities at 3.5, 5, and 8 MHz were in agreement with theoretical computations of this parameter for the phantom.

PACS numbers: 43.20.Gp, 43.35.Cg

INTRODUCTION

The effective scatterer number density[1] and its frequency dependence may be useful for ultrasonic tissue characterization. A data reduction method to determine a frequency dependent effective scatterer number density was presented in previous papers.[2,3] This method involves evaluating the ratio of the fourth moment to the square of the second moment of backscattered echo signals. The value of the effective scatterer number density and its statistical uncertainty are found after applying data reduction algorithms that account for experimental factors in this ratio. Previous experimental assessments of this method were applied to test phantoms containing small glass bead scatterers. Accurate measurements of the scatterer number density were reported for scatterer concentrations ranging from 134 to 750/cm^3.[2,3]

The present paper involves scatterer number density determinations in materials having more complex scattering properties. It has been shown that for tissues such as liver[4] and kidney[5] different structures dominate the scattering at different frequencies. Therefore, scatterer number density estimations in tissues may be reflective of this effect. Tests in a phantom with distributions of scatterer sizes, likely yielding effective scatterer number densities that depend on the dominant scatterer at a particular frequency, are reported here. Phantom tests yielded good agreement between the measured values of the frequency dependence of the effective scatterer number density and those calculated using first principles.

I. THEORY

Our data reduction method has been presented in detail previously,[2,3] so we will only briefly outline it here. We consider the situation where a pulsed transducer is used to insonify a medium containing scatterers. The same transducer serves as a receiver for echoes scattered from the medium. Randomly distributed discrete scatterers are assumed to give rise to echo signals. Over the surface of the transducer, the scattered wave from each scatterer is assumed to be spherically symmetric about the position of the scatterer.

Because of the random scatterer positions, the echo signal $V(t)$, or its Fourier transform $V(\omega)$ is a random variable. The latter quantity is represented by[2]

$$V_g(\omega)=\int_{-\infty}^{+\infty} d\omega'\ T(\omega')B(\omega')W(\omega-\omega') \times\sum_{i=1}^{M}\psi_i(\omega')A^2(\mathbf{r}_i,\omega'), \tag{1}$$

where $T(\omega)$ is a complex transfer function relating the net instantaneous force on the transducer at angular frequency ω to the detected voltage, $B(\omega)$ is a complex superposition coefficient corresponding to the frequency composition of the emitted pulse, $\psi_i(\omega)$ is the value of the angular distribution function[6] at a 180° scattering angle for the ith scatterer located at position $\mathbf{r}_i$, and $W(\omega'-\omega)$ is the Fourier transform of a gating function used to select echo signals from a particular region. The sum is over all scatterers, M, in the sample volume, $\Delta\Omega$. The volume is wide enough compared to the ultrasound beam, expressed as $A(\mathbf{r},\omega)$, and extends a sufficient distance axially to include all scatterers contributing to any significant degree to the gated echo signal segment.

Scatterer number density determinations are done using higher moments of the echo signals for situations in which a sparse number of scatterers are present in the sample volume. The number of scatterers in the sample volume can then be assumed to follow the Poisson distribution. For gate durations that are long compared to the period of the wave, the ratio of the fourth moment to the square of the second moment of the frequency domain echo signal is given by[2]

$$\frac{\langle (V_g(\omega)V_g^*(\omega))^2\rangle}{\langle V_g(\omega)V_g^*(\omega)\rangle^2}=2+\frac{1}{N_{\mathrm{eff}}(\omega)} \cdot\frac{\int\int\int_{\Delta\Omega}d\mathbf{r}|J(\mathbf{r},\omega)|^4}{\{\int\int\int_{\Delta\Omega}d\mathbf{r}|J(\mathbf{r},\omega)|^2\}^2}, \tag{2}$$

[a]Siemens Medical Systems, Inc., Issaquah, WA 98027-7002.

 0001-4966/96/99(4)/1932/5/$6.00

where $\langle\cdots\rangle$ stands for the expectation value, and

$$N_{\text{eff}}(\omega)\equiv\langle N\rangle\,\frac{\langle|\psi(\omega)|^2\rangle^2}{\langle|\psi(\omega)|^4\rangle} \tag{3}$$

is defined as the "effective scatterer number density" at angular frequency ω. The quantity is the actual scatterer number density $\langle N\rangle$ multiplied by the frequency-dependent factor $\langle|\psi(\omega)|^2\rangle^2/\langle|\psi(\omega)|^4\rangle$. The latter quantity depends on $|\psi(\omega)|^2\equiv\psi(\omega)\psi^*(\omega)$, which is the differential scattering cross section for each scatterer at frequency ω at a scattering angle of 180°. The quantity $J(\mathbf{r},\omega)$ is given by

$$J(\mathbf{r},\omega)\equiv\int_{-\infty}^{+\infty}d\omega'\;T(\omega')B(\omega')W(\omega-\omega')A^2(\mathbf{r},\omega'), \tag{4}$$

where the factors in the integrand are defined above. Thus the experimental conditions affecting the echo signal voltage, including the transducer field and the effects of the signal segmenting time gate, are explicitly accounted for.

If we define

$$Y(\omega)\equiv\frac{\langle(V_g(\omega)V_g^*(\omega))^2\rangle}{\langle V_g(\omega)V_g^*(\omega)\rangle^2}-2. \tag{5}$$

Equation (2) can be simplified to

$$N_{\text{eff}}(\omega)=Y(\omega)^{-1}\times V_{\text{eff}}(\omega)^{-1}. \tag{6}$$

Here the ratio of the volume integrals,

$$V_{\text{eff}}(\omega)\equiv\frac{\{\iiint_{\Delta\Omega}d\mathbf{r}|J(\mathbf{r},\omega)|^2\}^2}{\iiint_{\Delta\Omega}d\mathbf{r}|J(\mathbf{r},\omega)|^4}, \tag{7}$$

is an effective sample volume for this analysis. The magnitude of $V_{\text{eff}}(\omega)$ for typical experimental conditions is discussed in Sec. III.

Thus the effective scatterer number density is determined by computing the $Y(\omega)$ term in Eq. (5) and applying the data reduction formulation in Eq. (6). This approach has been verified using simple phantoms consisting of glass bead scatterers in gel.[2]

II. DETERMINATIONS OF $N_{\text{eff}}(\omega)$ VERSUS FREQUENCY

A. Scattering materials

Soft tissues are believed to involve more complex sets of scatterers than the situation represented in previous tests of this technique. For example, Nicholas suggests that liver tissue is dominated by two sets of scatterers, one being on the order of 1 mm in diameter, the other being on the order of 20–40 μm.[7] Each set would dominate the backscatter signals, and hence the quantity given in Eq. (5), at a different frequency.

To test the determination of an effective scatterer number density under these conditions, a phantom containing two types of scatterers was constructed (see Fig. 1). One type consists of 33-μm-diam glass beads randomly distributed. The other consists of agar/graphite spheres ranging from 0.85 to 1.15 mm in diameter. The number density for the 33-μm beads is 4×10^3 cm^{-3}, while that for the agar/graphite spheres is 50 cm^{-3}. These agar/graphite spheres consist of

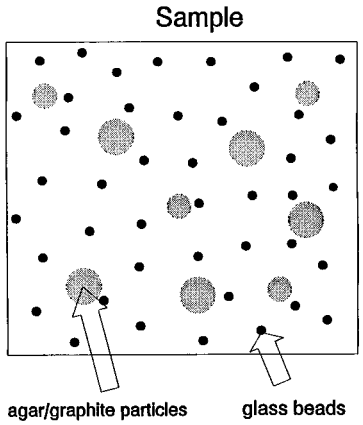

FIG. 1. Schematic drawing of the test phantom. It consists of 1.12-mm-diam agar/graphite sphere and 30-μm glass beads randomly distributed in a gel medium.

3% dry weight agar permeated with a uniform distribution of powdered graphite. The concentration of graphite powder is 60 mg/ml. The powdered graphite particles are small enough (the mean diameter is around 5 μm) that their contributions to scattering are derived only through increasing the mean density of the spheres relative to the surrounding media.

Size distributions of the scatterers in each set were measured using an optical microscope with a calibrated ocular micrometer. Results are shown in Figs. 2 and 3.

The backscatter coefficient and the effective scatterer number density can be calculated if required parameters of the scatterers and surrounding media are known. The parameters needed are the mass density (2.38 g/cm^3 for the glass beads, 1.036 g/cm^3 for the agar/graphite particles and 1.01 g/cm^3 for the surrounding material), Poisson's ratio (0.21 for glass beads and 0.50 for a fluidlike material) and the longitudinal speeds of sound (5572 m/s for the glass beads and 1540 m/s for the agar/graphite spheres and the surrounding gel in the phantom).

The differential scattering cross section per scatterer (agar sphere or glass bead) at angular frequency ω for a scattering angle of 180°, denoted by $|\psi_i(\omega)|^2$, was calculated

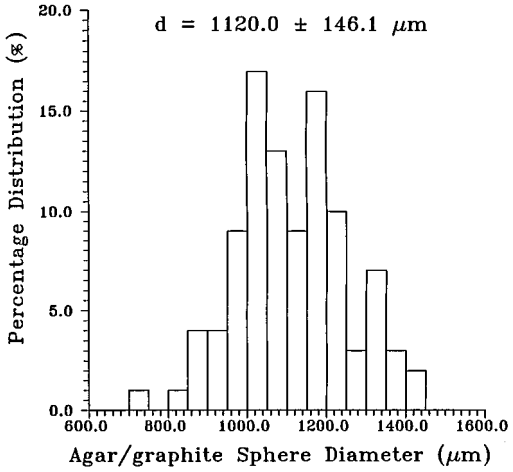

FIG. 2. Size distribution of the agar/graphite spheres in the test phantom.

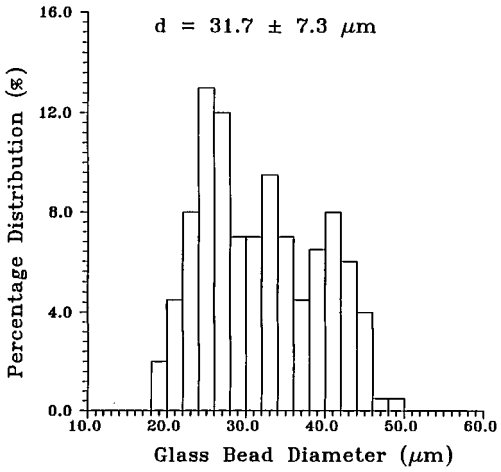

FIG. 3. Size distribution of the glass beads in the test phantom.

using expressions derived by Faran.[8] The mean and the mean-square values of the differential scattering cross section at 180° are given by

$$\langle|\psi(\omega)|^2\rangle \approx \sum_{i=1}^{L} L_i |\psi_i(\omega)|^2 \tag{8}$$

and

$$\langle|\psi(\omega)|^4\rangle \approx \sum_{i=1}^{L} L_i |\psi_i(\omega)|^4, \tag{9}$$

where L_i is the number fraction of scatterers in the ith diameter bin taken from Figs. 2 and 3, $|\psi_i(\omega)|^2$ is the differential scattering cross section for the scatterers of this diameter, and L is the number of bins. Then the theoretical predictions for both the backscatter coefficient and the effective scatterer number density in the test phantom are given by

$$\eta(\omega) = \langle N\rangle \langle|\psi(\omega)|^2\rangle \tag{10}$$

and

$$N_{\text{eff}}(\omega) = \langle N\rangle \frac{\langle|\psi(\omega)|^2\rangle^2}{\langle|\psi(\omega)|^4\rangle}, \tag{11}$$

where $\langle N\rangle$ is the actual scatterer number density.

The results of these predictions are shown in Figs. 4 and 5 for the test phantom. Figure 4 shows the expected backscatter coefficient for the glass beads only (dashed line) and the net backscatter coefficient for the phantom (solid line) when the agar spheres are indicated. Figure 5 presents corresponding predictions for the effective scatterer number density. $N_{\text{eff}}(\omega)$ is expected to be about 60.0 cm^{-3} at 3.5 MHz, 2.5×10^2 cm^{-3} at 5.0 MHz, and 1.75×10^3 cm^{-3} at 8.0 MHz, respectively. The anticipated result that the larger scatterers (agar/graphite spheres) dominate the backscatter signal at lower frequencies, while the smaller scatterers (fine glass beads) dominate at higher frequencies is seen in these predictions.

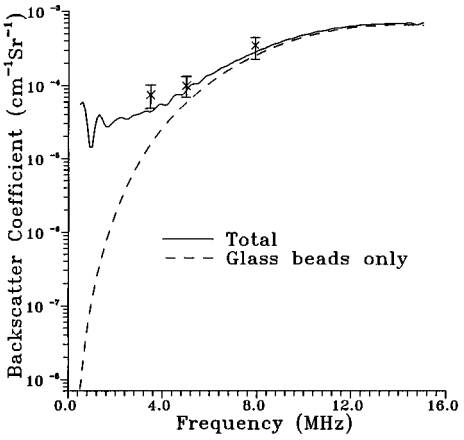

FIG. 4. Theoretical prediction of the backscatter coefficient in the test phantom, based on Eq. (9). The solid line shows the backscatter coefficient for the composite material, while the dashed curve shows the contribution to the backscatter coefficient by the glass beads only. Three additional points × are experimental determinations of the backscatter coefficient.

B. Experimental procedure

Experimentally, three focused transducers with central frequencies of 3.5, 5.0, and 8.0 MHz were used to record echo signals from the test phantom. The transducers have a single quarter wavelength impedance matching layer on the outside surface of the piezoelectric crystal to improve transmission into waterlike substances. To calculate $A(\mathbf{r},\omega)$, the pressure distribution for each focused transducer, it is necessary to know the effective aperture and radius of curvature (ROC) of their active elements.[9,10] As shown before,[11] the directivity function for a focused transducer accurately describes the relative amplitude in the ''focal plane'' of the transducer driven by single frequency signals. The focal plane is defined as a plane perpendicular to the axis of symmetry of the radiating element and passing through its center of curvature. Agreement of the pressure distribution with the directivity function is unique to this plane, and this fact can

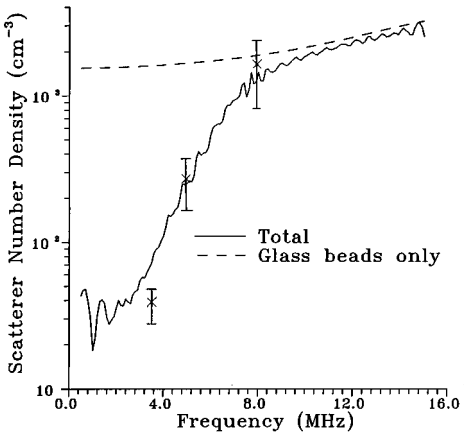

FIG. 5. Theoretical prediction of the effective scatterer number density for the test phantom, based on Eq. (10). The solid line shows the predicted effective scatterer number density for the composite material, while the dashed curve shows the predicted effective scatterer number density for the glass beads alone. Three additional points × are experimental results for the effective scatterer number density.

TABLE I. Values of the radius of curvature (ROC) and the effective aperture for the three transducers used to record echo data from the phantom.

Nominal resonant frequency (MHz)	Radius of curvature (cm)	Effective aperture (mm)
3.5	9.65±0.07	19.2±0.02
5.0	8.50±0.06	18.6±0.02
8.0	5.42±0.02	16.0±0.02

be used to determine experimentally the radius of curvature and the effective aperture.[12] The pressure field of the transducer is scanned with a pointlike hydrophone searching for the plane which yields the best approximation to the directivity function. The distance between the first-axis minima defining the mainlobe of the beam are then used to estimate the effective transducer aperture. Experience has shown that the transducer radius of curvature can be determined to within 0.7 percent, and the lateral distance between off-axis minima to within 0.2 mm.[12] By propagating uncertainties, this corresponds to a 0.1 to 0.2 mm uncertainty in the transducer aperture.[13] Table I lists the values of these two parameters as well as their uncertainties for each transducer.

Transducers were excited with single cycle pulses whose frequency was chosen to be the nominal frequency of the transducer. The effective scatterer number density determination involves recording two types of echo signals. First, the echo from a planar reflector submerged in water and oriented with its reflecting surface perpendicularly to the incident ultrasound beam was employed to determine the system-dependent factor, $T(\omega)B(\omega)$.[14] Then backscattered echo signals from the test phantom were recorded at 400 statistically independent positions by lateral translations of the phantom between recordings. Echo signals from a depth of 0.75 cm into the phantom were isolated using a 5-μs rectangular gate.

Discrete Fourier transforms of each of these 400 truncated waveforms were then computed, yielding the values of $V_g(\omega)$. The average values of $V_g(\omega)V_g^*(\omega)$ and $[V_g(\omega)V_g^*(\omega)]^2$ were computed for the data from the test phantom; these are denoted by $\langle\langle V_g(\omega)V_g^*(\omega)\rangle\rangle$ and $\langle\langle[V_g(\omega)V_g^*(\omega)]^2\rangle\rangle$. The value of

$$\Lambda(\omega)=\frac{\langle\langle[V_g(\omega)V_g^*(\omega)]^2\rangle\rangle}{\langle\langle V_g(\omega)V_g^*(\omega)\rangle\rangle^2}-2$$

was determined over the frequency bandwidth for each transducer. Even for 400 experimental samples, $\Lambda(\omega)$ is a poor approximation of $Y(\omega)$. The uncertainty can be reduced either by increasing the number of samples or curve-fitting $\Lambda(\omega)$ over the frequency bandwidth for each transducer. Here the later course has been used.[2] Third-order polynomial curves were fit to the $\Lambda(\omega)$ values over 2.0-, 3.0-, and 4.5-MHz bandwidths for the 3.5-, 5.0-, and 7.5-MHz transducers. The polynomial curves were then used to determine the experimental values of $N_{\text{eff}}(\omega)$ at the center frequencies of the transducers. Standard deviations were calculated using the mean square deviation of $\Lambda(\omega)$ from the polynomial fits, averaged over the frequency bandwidth.

TABLE II. Experimental results for the effective scatterer number densities, $N_{\text{eff}}(\omega)$, and the backscatter coefficient, $\eta(\omega)$, for the test phantom. The effective sample volume for each experimental frequency is listed in row 2.

Ultrasound frequency (MHz)	3.5	5.0	8.0
Effective sample volume$\times10^{-3}$ (cm^3) (5-μs gate)	20.0	7.45	1.19
$Y(\omega)$	0.73±0.2	1.9±0.8	1.8±0.8
$N_{\text{eff}}(\omega)$ (cm^{-3})	37±10	(2.6±1.0)×10^2	(1.5±0.7)×10^3
$\eta(\omega)$ (cm^{-1} Sr^{-1})	(7.2±2.7)×10^{-5}	(9.8±3.0)×10^{-5}	(3.5±1.2)×10^{-4}

III. RESULTS AND DISCUSSION

As shown in Figs. 4 and 5, and as well as in Table II, the experiments using different transducers yielded results for both the backscatter coefficients and the effective scatterer number densities that were in reasonable agreement with theoretically predicted values. Measured backscatter coefficients (Fig. 4) agree with predicted backscatter coefficients to within the error bars, and except for the 3.5-MHz value, the same can be said for the effective scatterer number density measurements. At 3.5 MHz, we recorded an effective scatterer number density of (37±10) cm^{-3}, whereas the expected value is 58 cm^{-3}. At 8.0 MHz, the measured and expected effective scatterer number densities are (1.5±0.7)×10^3 cm^{-3} and 1.75×10^3 cm^{-3}, respectively. The data follow the anticipated result that the large scatterers (agar/graphite spheres) dominate the backscatter signals and the effective scatterer number density at a lower frequency (3.5 MHz), whereas the smaller scatterers (glass beads) dominate the backscatter signals and the effective scatterer number density at a higher frequency (8.0 MHz).

The difference between the ''experimental'' and ''theoretical'' results may be caused by either experimental errors or by the uncertainties of the parameters used to calculate the theoretical values. For example, the speed of sound in agar/graphite was assumed to be the same as that in the background medium, and the mass density for the agar/graphite spheres was estimated at 1.036 g/cm^3. If instead a density of 1.05 g/cm^3 is used for the agar/graphite spheres, this causes at least a 35% decrease in the theoretical result for the effective scatterer number density (about 38 cm^{-3}) and at least a factor of 2 increase in the theoretical result for the backscatter coefficient at 3.5 MHz, because of a greater scattering contribution from the large spheres. The uncertainty in the mass density estimation for the agar/graphite spheres comes mainly from the volume determinations. At best, the volume reading uncertainties were ±0.2 ml. Because a volume difference was used, this translates into an uncertainty of ±0.3 ml, or ±0.2% of the 150-ml volume. Thus the uncertainty in the mass density determination could easily be ±0.2%.[15]

As shown in a previous paper,[3] the standard deviation of the effective scatterer number density depends mainly on the average number of scatterers contributing to the time-gated echo signal. This in turn depends on the effective sample volume defined in Eq. (7). Note $V_{\text{eff}}(\omega)$ is not the same as the resolution cell volume defined for B-mode imaging.[16] For an example, for our 3.5-MHz transducer near the focal region,

the resolution cell volume is approximately 1.6 mm^3, while the effective sample volume is around 20 mm^3. A transducer, with a smaller focal spot was necessary to measure the scatterer number density at 8 MHz, because a relative small effective sample volume yields a smaller statistical uncertainty.

The effective scatterer number density is fundamentally related to tissue microstructure. Any method for extracting this parameter from backscatter echo data must account for measurement system dependencies on the data. In applications involving tissues, where the effective scatterer number density is unknown, iterative methods guided by scatterer number densities estimated histologically may be necessary. This approach seemed to yield a reasonable result for the scatterer number density of microscopic structures in pig liver.[1] Obviously, much more work is needed to understand and apply these methodologies to tissue.

IV. SUMMARY AND CONCLUSIONS

An expression for determining a frequency-dependent effective scatterer number density was evaluated using a special phantom. The phantom contained two scatterer types, each dominating the scattering in a specific ultrasound frequency range. Measurement results agreed with theoretical predictions, showing the effective scatterer number density estimate depends on the dominant scatterers at the analysis frequency.

ACKNOWLEDGMENTS

The assistance of Mr. Gary Frank in constructing the phantom is greatfully acknowledged. This work was support in part by NIH Grant No. R01-CA39224 and by a UW Medical Physics, Richard B. Mazess Advanced Fellowship.

[1] G. F. Sleefe and P. P. Lele, ''On estimating the number density of random scatterers from backscattered acoustic signals,'' Ultrasound Med. Biol. **14**, 709–727 (1988).
[2] J. F. Chen, E. L. Madsen, and J. A. Zagzebski, ''A method of determination of the frequency dependent effective scatterer number density,'' J. Acoust. Soc. Am. **95**, 77–95 (1994).
[3] J. F. Chen, E. L. Madsen, and J. A. Zagzebski, ''Statistical uncertainty in estimates of an effective scatterer number density,'' J. Acoust. Soc. Am. **96**, 2556–2563 (1994).
[4] J. C. Bamber and C. R. Hill, ''Acoustic properties of normal and cancerous liver: Dependence on pathological condition,'' Ultrasound Med. Biol. **7**, 121–133 (1981).
[5] M. F. Insana, ''Modeling acoustic backscatter from kidney microstructure using an anisotropic correlation function,'' J. Acoust. Soc. Am. **97**, 649–655 (1995).
[6] P. M. Morse and K. U. Ingard, *Theoretical Acoustics* (McGraw-Hill, New York, 1968), Chap. 8.
[7] D. Nicholas, C. R. Hill, and D. K. Nassiri, ''Evaluation of backscattering coefficient for excised human tissues: Principle and techniques,'' Ultrasound Med. Biol. **8**, 7–15 (1982).
[8] J. J. Faran, Jr., ''Sound scattering by solid cylinders and spheres,'' J. Acoust. Soc. Am. **23**, 405–418 (1951).
[9] E. L. Madsen, M. M. Goodsitt, and J. A. Zagzebski, ''Continuous waves generated by focused radiators,'' J. Acoust. Soc. Am. **70**, 1508–1517 (1981).
[10] M. M. Goodsitt, E. L. Madsen, and J. A. Zagzebski, ''Field patterns of pulsed focused ultrasonic radiators in attenuating and nonattenuating media,'' J. Acoust. Soc. Am. **71**, 318–329 (1982).
[11] H. T. O'Neil, ''Theory of focusing radiators,'' J. Acoust. Soc. Am. **21**, 516–526 (1949).
[12] T. J. Hall, ''Experimental methods for accurate determination of acoustic backscatter coefficient,'' Ph.D. thesis, University of Wisconsin—Madison, 1988.
[13] P. B. Bevington, *Data Reduction and Error Analysis for Physical Science* (McGraw-Hill, New York, 1969).
[14] E. L. Madsen, M. F. Insana, and J. A. Zagzebski, ''Method of data reduction for accurate determine of acoustic backscatter coefficients,'' J. Acoust. Soc. Am. **76**, 913–923 (1984).
[15] R. B. Chin, E. L. Madsen, J. A. Zagzebski, H Jadvar, X. K. Wu, and G. R. Frank, ''A reusable perfusion supporting tissue-mimicking material for ultrasound hyperthermia phantoms,'' Med. Phys. **17**, 380–390 (1990).
[16] R. F. Wagner, M. F. Insana, and S. W. Smith, ''Fundamental correlation lengths of coherent speckle in medical ultrasound images,'' IEEE Trans. Sonics Ultrason. **35**, 34–44 (1988).